Optimization of the propulsion of a flapping airfoil by kinematic control

Houssam Soueid, Alessandro Bottaro & Laura Guglielmini

DICAT, Università di Genova
1 Via Montallegro, 16145 Genova Italy
houssam.soueid@unige.it

Abstract :

The propulsion of a two-dimensional flapping airfoil is optimized by controlling the kinematics of its motion for an MAV application. The optimization is done numerically through the resolution of flow and sensitivity equations for an incompressible low-Reynolds number configuration. The gradient of a chosen functional, related to the efficiency, is deduced and used to update the control parameters via a steepest-descent method. The results show the ability of the method to find precisely the optimal kinematics despite the effort required to optimize the choice of the spatio-temporal grid. Results confirm the optimality of a phase lag close to 90^o between pitching and heaving and show a relatively higher sensitivity with respect to the pitching amplitude compared to the other control parameters.

Résumé :

La propulsion d'une aile battante bidimensionnelle, applications liées aux micro-drones, est optimisée en contrôlant numériquement sa cinématique à travers la résolution des équations du mouvement et des sensibilités d'un écoulement incompressible à faible nombre de Reynolds. Le gradient de la fonctionnelle choisie est déduit et utilisé pour actualiser la valeur des paramètres de contrôle par la méthode de la plus grande pente. Les résultats montrent la capacité de la méthode à trouver d'une manière précise le mouvement optimal de l'aile malgré les difficultés liées au bon choix du maillage et du pas de temps. On confirme qu'un déphasage, entre l'oscillation verticale et le tangage, voisin de 90^o est optimal et on montre que la sensibilité par rapport à l'amplitude du tangage est relativement plus élevée que celle des autres paramètres de contrôle.

Key-words :

Flapping airfoil; Sensitivity optimization; Numerical simulation

1 Introduction

The progress accomplished in the miniaturization of electronic and mechanical devices has rendered possible the realization of small autonomous airplanes during the last two decades. These micro air vehicles (MAV) of 20 cm wingspan flying at speeds close to 50 km/h have attracted much attention due to their broad range of civil and military applications (spying, studies of the atmosphere, surveillance ...), to their easy and fast deployment, low cost, stealth, etc. (Hewish (1997), Canan (1999)). A large number of studies has been aimed recently at the understanding of the mechanisms of drag reduction and stall delay developed by fish and birds (Rayner (1988), Spedding *et al*. (1995)). The desire to mimic the motion of birds has been encouraged by a number of papers showing that at MAV's scale, flapping flight can be more efficient than the fixed wings counterpart (Kroo *et al*. (2001)).

The main limitation of MAV's at present is their small autonomy, typically between thirty minutes and one hour. Improving the duration of MAVs' missions requires progress in the conception of the propulsive system used, *i.e.* better batteries and motors. The improvement can also be accomplished by increasing the efficiency of the flight (measured by the ratio of the useful power to the total required power) by acting directly on the kinematics of the wings. This approach is adopted in the present work. Several authors (Triantafyllou *et al*. (1993), Wang (2000), Lewin *et al*. (2003), Guglielmini *et al*. (2004)) showed, by exploring the space of parameters, that the efficiency of flapping can be optimal for some values of the relevant parameters. Here, we aim at finding optimal flight regimes by solving the sensitivity equations and by driving to zero the gradient of an efficiency-related functional.

Once the optimal kinematics is found, we relate our results to those by Triantafyllou *et al*. (1993) and Isogai *et al*. (1999) on the optimal Strouhal number and phase between pitching and heaving motions. Inspection of the sensitivity fields should provide clues on the regions of space where flow control is more efficient.

2 Governing equations

The flow is computed around a flapping two-dimensional airfoil. The incompressibility of the flow allows to eliminate the pressure and to reduce the dimension of the problem by introducing two variables: the vorticity ω and the stream function ψ.

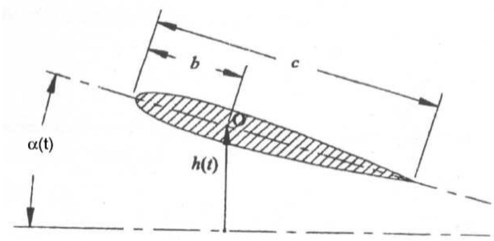

Figure 1: Definition of the flapping motion.

The airfoil is transformed into a circle via a Joukowski transformation. The flow equations are then solved in a moving reference frame, fixed with the airfoil, and this renders the boundary conditions on the airfoil easy to impose.

We consider the angular frequency of flapping σ^* and the chord length c^* as relevant scales for time and length, and this leads to the following dimensionless equations for ψ and ω:

$$\left\{ \begin{array}{l} \frac{\partial \omega}{\partial t} + \frac{1}{\sqrt{J}}\left[v_r \frac{\partial \omega}{\partial r} + \frac{v_\theta}{r}\frac{\partial \omega}{\partial \theta}\right] = \frac{1}{ReJ}\left[\frac{\partial^2 \omega}{\partial r^2} + \frac{1}{r}\frac{\partial \omega}{\partial r} + \frac{1}{r^2}\frac{\partial^2 \omega}{\partial \theta^2}\right], \\ \frac{\partial^2 \psi}{\partial r^2} + \frac{1}{r}\frac{\partial \psi}{\partial r} + \frac{1}{r^2}\frac{\partial^2 \psi}{\partial \theta^2} = -J\omega, \end{array} \right. \tag{1}$$

where

$$\begin{array}{l} v_r = \frac{1}{\sqrt{J}}\left[\frac{1}{r}\frac{\partial \psi}{\partial \theta} - \left(\dot{h}sin(\alpha) - \dot{\alpha}Y\right)\left(\frac{\partial X}{\partial \xi}cos\theta + \frac{\partial X}{\partial \chi}sin\theta\right) - \left(\dot{h}cos(\alpha) + \dot{\alpha}X\right)\left(\frac{\partial Y}{\partial \xi}cos\theta + \frac{\partial Y}{\partial \chi}sin\theta\right)\right] \\ v_\theta = \frac{1}{\sqrt{J}}\left[-\frac{\partial \psi}{\partial r} - \left(\dot{h}sin(\alpha) - \dot{\alpha}Y\right)\left(\frac{\partial X}{\partial \chi}cos\theta - \frac{\partial X}{\partial \xi}sin\theta\right) - \left(\dot{h}cos(\alpha) + \dot{\alpha}X\right)\left(\frac{\partial Y}{\partial \chi}cos\theta - \frac{\partial Y}{\partial \xi}sin\theta\right)\right] \end{array}$$

The dots denote derivation with respect to time t, (X, Y) are the coordinates in the Cartesian frame based on the airfoil, (ξ, χ) are the transformed coordinates in the Joukowski plane, J is the Jacobian between these two frames, (r, θ) are the polar coordinates in the transformed plane and Re is the Reynolds number defined by $Re = \frac{\sigma^* c^2}{16\nu^*}$, with ν^* the kinematic viscosity of the fluid. The boundary conditions are written in terms of ψ and ω, and the velocity is imposed equal to U^*_∞ and 0 on the outflow boundary and on the airfoil, respectively; the equations are marched in time starting from an initial condition of vanishing vorticity and stream function.

3 Kinematics and control parameters

The motion imposed to the airfoil is a combination of harmonic oscillations of translation and rotation described by the equation (2).

$$\left\{\begin{array}{l} h\left(t\right)=\sum_{k=1}^{N}h_k sin(kt+\tau_k),\\ \\ \alpha\left(t\right)=\bar{\alpha}+\sum_{k=1}^{N}\alpha_k sin\left(kt+\phi_k\right). \end{array}\right. \tag{2}$$

We focus more particularly on the case $\bar{\alpha}=0$ and $\tau_k=0$. The configuration $N=1$ is usually assumed to mimic the motion of the fins of fish and the wings of birds. The same frequency is imposed for both oscillations. Under these conditions, the control parameters are the heaving amplitudes $(h_1, h_2, ...h_N)$, the pitching amplitudes $(\alpha_1, \alpha_2, ...\alpha_N)$ and the phases $(\phi_1, \phi_2, ...\phi_N)$. The letter g will be used in the following to denote one generic control parameter.

For any value of N, the period of the motion of the airfoil is equal to 2π. The numerical simulations showed that the transients generally last about two periods of oscillations, after which periodic states are achieved. Therefore, the equations are solved for two periods in time and the mean quantities are averaged during the last period. The time-marching is done with an ADI method where every temporal step is divided in two sub-steps, each one treating the equations in the r or θ directions. The size of the computational domain is typically between 10 and 20 chord lengths, in which roughly 500 000 nodes are distributed. A logarithmic distribution is used in the radial direction in order to better solve the boundary layer, whereas a uniform distribution is adopted for the angular direction. The dimensionless time step is typically between 10^{-4} and 10^{-3} and the classical Reynolds number $(Re_c=\frac{U^*_\infty c^*}{\nu^*})$ is taken of order 1000.

4 Sensitivities

The derivatives of ψ and ω with respect to the control variables are called sensitivities. They allow to determine the regions of the flow where control has a major effect and to compute the gradient of the cost functional. Hence, the derivative of the flow equations (1) yields the sensitivity equations:

$$\left\{\begin{array}{l} \frac{\partial\omega_{,g}}{\partial t}+\frac{1}{\sqrt{J}}\left[v_r\frac{\partial\omega_{,g}}{\partial r}+\frac{v_\theta}{r}\frac{\partial\omega_{,g}}{\partial\theta}+\frac{\partial v_r}{\partial g}\frac{\partial\omega}{\partial r}+\frac{1}{r}\frac{\partial v_\theta}{\partial g}\frac{\partial\omega}{\partial\theta}\right]=\frac{1}{ReJ}\left[\frac{\partial^2\omega_{,g}}{\partial r^2}+\frac{1}{r}\frac{\partial\omega_{,g}}{\partial r}+\frac{1}{r^2}\frac{\partial^2\omega_{,g}}{\partial\theta^2}\right]\\ \frac{\partial^2\psi_{,g}}{\partial r^2}+\frac{1}{r}\frac{\partial\psi_{,g}}{\partial r}+\frac{1}{r^2}\frac{\partial^2\psi_{,g}}{\partial\theta^2}=-J\omega_{,g} \end{array}\right. \tag{3}$$

where

$$v_{r,g}=\frac{1}{\sqrt{J}}\left[\frac{1}{r}\frac{\partial\psi_{,g}}{\partial\theta}-\left(\dot{h}sin(\alpha)-\dot{\alpha}Y\right)_{,g}\left(\frac{\partial X}{\partial\xi}cos\theta+\frac{\partial X}{\partial\chi}sin\theta\right)-\left(\dot{h}cos(\alpha)+\dot{\alpha}X\right)_{,g}\left(\frac{\partial Y}{\partial\xi}cos\theta+\frac{\partial Y}{\partial\chi}sin\theta\right)\right]$$
$$v_{\theta,g}=\frac{1}{\sqrt{J}}\left[-\frac{\partial\psi_{,g}}{\partial r}-\left(\dot{h}sin(\alpha)-\dot{\alpha}Y\right)_{,g}\left(\frac{\partial X}{\partial\chi}cos\theta-\frac{\partial X}{\partial\xi}sin\theta\right)-\left(\dot{h}cos(\alpha)+\dot{\alpha}X\right)_{,g}\left(\frac{\partial Y}{\partial\chi}cos\theta-\frac{\partial Y}{\partial\xi}sin\theta\right)\right]$$

Compared to the flow equations, the sensitivity equations have a source term due to the dependency of v_r and v_θ on g. The system is uncoupled since for $t=t^n$, the equation for ω_g is first solved with an ADI method using ψ_g at $t=t^{n-1}$; once ω_g is known at $t=t^n$, we inject it in the second equation to compute ψ_g. The boundary conditions for the sensitivities are obtained by deriving the flow boundary conditions with respect to the control parameters.

5 Cost functional and gradient

The efficiency of flight, η, is the ratio of the useful power for flying to the total power required. The cost functional to be minimized is thus:

$$\Upsilon = \beta^2 \bar{P} + \gamma^2 \bar{F} U_\infty + \delta^2 \frac{1}{2\pi} \int_0^{2\pi} \alpha^2(t)dt + \epsilon^2 \frac{1}{2\pi} \int_0^{2\pi} h^2(t)dt \tag{4}$$

where

$$\begin{cases} \bar{P} = \frac{-1}{2\pi} \int_0^{2\pi} F_X sin(\alpha(t))\dot{h}(t)dt - \frac{1}{2\pi} \int_0^{2\pi} F_Y cos(\alpha(t))\dot{h}(t)dt - \frac{1}{2\pi} \int_0^{2\pi} M_Z \dot{\alpha}(t)dt, \\ \bar{F} = \frac{1}{2\pi} \int_0^{2\pi} F_X cos(\alpha(t))dt - \frac{1}{2\pi} \int_0^{2\pi} F_Y sin(\alpha(t))dt, \end{cases}$$

are the mean power required to move the airfoil and the mean horizontal force in the laboratory reference. The negative or positive value of this force indicates whether the airfoil is mainly producing thrust or drag, respectively. The third and the fourth terms in the functional (4) are added in order to limit the cost of the control, thus preventing the optimal kinematics from diverging. Furthermore, the non-dimensional value of U_∞ is computed as $U_\infty = \frac{1}{fr}$ where fr is the reduced frequency defined as $fr = \frac{c^*\sigma^*}{4U_\infty^*}$ when the airfoil is translating in the horizontal direction (not hovering). In the present work, we choose $fr = 0.3665$ leading to $U_\infty = 2.73$. Multiplying the horizontal force by the velocity at infinity allows to include the required and the useful powers in the cost functional; it also prevents finding the minimum of the functional for a motionless airfoil ($\bar{P} = 0$) if $\beta^2 = \gamma^2$ or for an airfoil which dissipates the energy of the flow into drag ($\bar{P} < 0$) when $\beta^2 < \gamma^2$.

6 Results

Before exploring the sensitivity fields, we start with the validation of the gradient computation. Therefore, we compare the value of the gradient computed with the sensitivity method to the gradient estimated by a simple finite difference method and we ensure a vanishing gradient when the minimum of the functional is reached. The plots in figure 2 for $N = 1, Re_c = 1100, \alpha_1 = -25°$, $\phi_1 = 90°$ and $(\beta^2, \gamma^2, \delta^2, \epsilon^2) = (1, 2, 1, 1)$ show a very satisfactory agreement. We notice that the optimal solution is found for a thrust producing flapping airfoil. The same kind of results can be obtained if we control α_1 or ϕ_1, fixing the other two parameters, or if we control all the three parameters successively. The difficulty lies in the choice of the computational domain and the grid, since the gradient turns out to be very sensitive to such choices. To drive the gradient to zero a steepest descent method is adopted. It allows to locate roughly the optimal conditions after a few iterations.

We confirm here the results obtained by Isogai *et al.* (1999) who showed that the highest efficiency occurs when the pitch oscillation leads the heave oscillation by an angle close to 90°. As a matter of fact, the cost functional considered in the present work is minimal for $\phi_1 = 87.302°$ when $(h_1, \alpha_1) = (3, -35°)$ and for $\phi_1 = 81.947°$ when $(h_1, \alpha_1) = (2, -25°)$. This high efficiency is related to the fact that the region of separated flow remains confined to a small neighborhood of the trailing edge. On the other hand, figure 3, where the opposite of the efficency $(-\eta)$ is plotted versus the heaving amplitude, shows that the minimum of the cost corresponds quite closely to conditions of maximal efficency. A snapshot of the vorticity field and its sensitivity with respect to h_1 is shown in figure 4. All the sensitivity fields are similar. They appear to be formed by layered structures of high and low sensitivity functions in the wake of the airfoil; however, the largest magnitudes are found in close proximity of the airfoil.

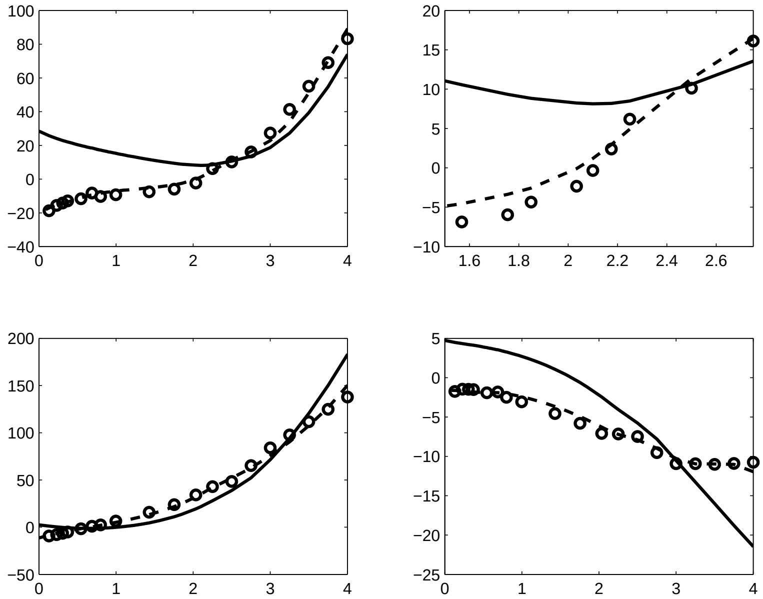

Figure 2: Validation of the gradient computation. Top-left: the cost functional, top-right: zoom of the cost functional, bottom-left: the mean required power, bottom-right: the mean horizontal force. Solid lines denote the function, dashed lines its gradient computed with sensitivity method with comparison to the 2^{nd} order finite-difference method (circles).

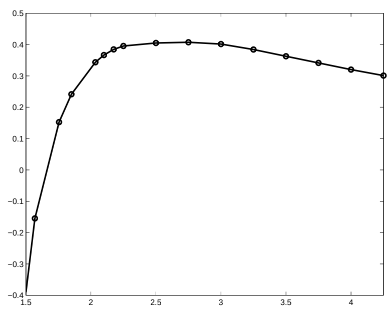

Figure 3: The effect of the heaving amplitude on the efficiency $(-\eta)$ for $\alpha_1 = -25°$ and $\phi_1 = 90°$.

7 Conclusions

The optimal propulsive properties of a two-dimensional flapping airfoil are examined numerically with the technique of flow sensitivities. The results show the ability of the method to identify the minimum of a given functional associated to the efficiency of the flight. The optimal value found are in agreement with the values found in the literature by extensive exploration of the space of parameters; the functional chosen here appears to be closely correlated to the efficiency of flight. The present work is being extended to a higher number of harmonics, to ver-

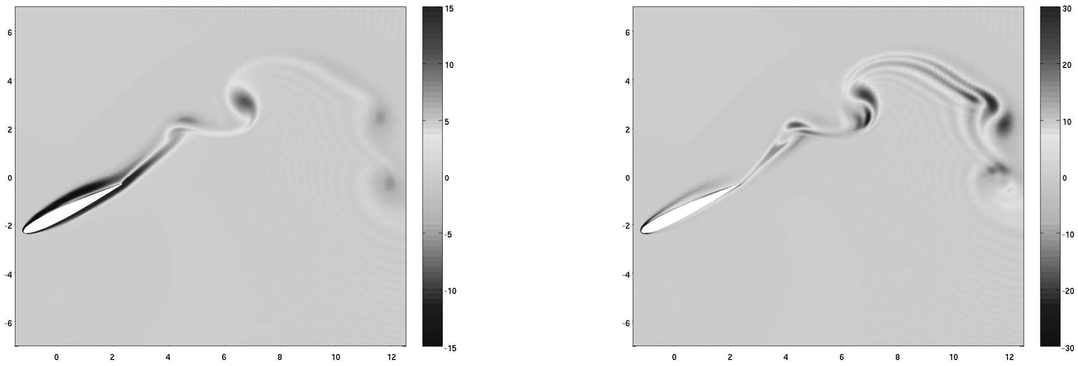

Figure 4: Vorticity field (left) and its sensitivity fields with respect to h_1 (right) at t=10.

ify the conjecture that a richer kinematics can yield high values of the thrust with an acceptable efficiency (Read *et al*. (2003)).

References

Canan, J.W. 1999 Seeing more, and risking less, with UAVs. *Aerospace America,* October, pp. 26-31

Guglielmini, L. and Blondeaux, P. 2004 Propulsive efficiency of oscillating foils. *European Journal of Mechanics. B/Fluids*, **23**, No. 2, 255-278

Hewish, M. 1997 Building a bird's-eye view for the battlefield. *Jane International Defense Review* , February, pp. 55-61

Isogai, K., Shinmoto, Y. and Watanabe, Y. 1999 Effects of dynamic stall on propulsive efficiency and thrust of flapping foil. *AIAA Journal* , **37**, No. 10, 1145-1151

Kroo, I., Kunz, P. 2001 Mesoscale flight and miniature rotorcraft development. *Fixed and flapping wing aerodynamics for micro air vehicle applications. Progress in Astronautics and Aeronautics*, (ed. T.J. Mueller) **195**, 503-517

Lewin, G.C. and Haj-Hariri, H. 2003 Modelling thrust generation of a two-dimensional heaving airfoil in a viscous flow. *Journal of Fluid Mechanics*, **492**, 339-362

Rayner, J.M.V. 1988 Form and function in avian flight. *Current Ornithology* , **5**, 1-77

Read, D.A., Hover, F.S. and Triantafyllou, M.S. 2003 Forces on oscillating foils for propulsion and maneuvering. *Journal of Fluids and Structures*, **17**, No. 1, 163-183

Spedding, G.R. and DeLaurier, J.D. 1995 Animal and ornithopter flight. *Handbook of Fluid Dynamics and Fluid Machinery*, (eds. J.A. Schetz and A.E. Fuhs) Wiley, New York.

Triantafyllou, G.S., Triantafyllou, M.S. and Grosenbaugh, M.A. 1993 Optimal thrust development in oscillating foils with application to fish propulsion. *Journal of Fluids and Structures*, **7**, 205-224

Wang, Z.J. 2000 Vortex shedding and frequency selection in flapping flight. *Journal of Fluid Mechanics*, **410**, 323-341